Egypt. J. Chem. **Vol. 66,** No. 6 pp. 31 - 39 (2023)

Egyptian Journal of Chemistry

http://ejchem.journals.ekb.eg/

New trend on antimicrobial activity of green AgNPs from *Trogoderma granarium* larval extract against antibiotic-resistant *Salmonella* Typhi

Marwah T. Alnuaimi[a], Zahraa Zahraw Aljanabi[b], Manal M. Adel*[c], Marwa Ahmed[d]

[a] *Department of Environment Technology and Water Technology Researches, Division of Pollution Treatment Technology, Ministry of Science and Technology, Baghdad 10001, Iraq*

[b] *Environment Research Center/ University of Technology, Baghdad 10001, Iraq*

[c] *National Research Centre, Pests & Plant Protection Dep. Agriculture institute, Cairo, EGYPT*

[d] *Biology Department, College of Science for Women, University of Baghdad, Iraq.*

Abstract

The development of green nanotechnology become very interest among researchers in order to synthesis eco-friendly of bio-nanoparticles. The current work used *Trogoderma granarium* larval extract as both a capping and reducing agent, as well as water as a solvent to biosynthesise stable silver nanoparticles (AgNPs). These biosynthesized nanoparticles were characterized with the help of atomic absorption spectroscopy (AAS UV–vis spectrophotometer), Zeta potential, Fourier infrared spectroscopy (FTIR), and atomic forced microscopy (AFM). It has been noted that within 5 minutes of reaction time, *T. granarium* larval extract can convert silver ions to silver nanoparticles. The antimicrobial activity of the AgNPs was screened against clinical isolate of multidrug-resistant *Salmonella* Typhi and showed inhibiting activities against *Salmonella* Typhi. As a result, this process may be utilized to produce rapid and eco-friendly stable silver nanoparticles with a size range of 59 nm which have antibacterial activity, suggesting that they could be exploited in the medical field.

Key words: Silver nanoparticles*; Trogoderma granarium* larval extract*; Salmonella* Typhi*;* antibiotic-resistant bacteria.

1. Introduction

In recent years, the rising spread of bacterial infections and the emergence of antimicrobial resistance have been identified as important concerns for the twenty-first-century biomedicine area, which necessitates the creation of innovative antibacterial drugs. One of the most active study fields in current materials science is nanotechnology [1].

Nanotechnology has also received a remarkable amount of interest in advanced fields of biology, physics, and chemistry. Nanoparticles, which may be of any shape, have at least one dimension of 100 nm or less [2].

The main benefits of NPs over larger-sized particles are their higher surface energy, unique magnetic characteristics [3]. NPs have a high surface-to-volume ratio due to their small size which made this property is extremely helpful in applications such as antifungal and antimicrobial activities [4]. A variety of procedures can be used to create nanoparticles, including physical, chemical, and biological (green) methods [5]. Physical methods in NPs fabrication are costly due the waste of energy, required a great temperature and pressure, and the need for very advanced equipment [6]. In the chemical synthesis of NPs, the generation of hazardous by-products is highlighted, and the use of certain chemicals is expensive and may result in the formation of toxic chemicals on the surface of NPs, which may introduce adverse effects on the environment [7] .While the biological approach is based on natural principles and includes a natural event that occurs in biological systems [8]. Where the biological technique used to produced NPs can called "green nanotechnology" and has sparked a lot of curiosity, where involved extract-mediated synthesis, particularly that using insect larval extracts, has been shown to be a very efficient and clean way among numerous biological methods for NPs synthesis[9].

Antibacterial mechanisms of NPs required that NPs must be in contact with bacterial cells in order to accomplish their antibacterial function. There are several forms of contact include electrostatic attraction,86 van der Waals forces (attraction of intermolecular forces between molecules)[10], hydrophobic interactions [11],

*Corresponding author e-mail: mhassanein11@hotmail.com (+2 01224214021)

Receive Date: 01 June 2022, Revise Date: 06 August 2022, Accept Date: 11 September 2022

DOI: 10.21608/EJCHEM.2022.142238.6216

receptor–ligand [12]. NPs then cross the bacterial cell membrane and assemblage along the metabolic pathway, influencing the function and shape of the bacterial cell membrane. Then, NPs interact with the basic components of bacterial cell's, such as DNA, ribosomes, lysosomes, and enzymes, causing different mode of alternations like; changes in cell membrane permeability, electrolyte balance disorders, oxidative stress, heterogeneous alterations, protein deactivation, enzyme inhibition, and changes in gene expression [13].

It has been advised to employ metal ions, such as Cu, Ag, and Au, in the treatment of many species of microorganisms, including $Gram^+$ and $Gram^-$ bacteria, as well as fungus [14]. Silver has a high toxicity against a wide variety of pathogens, and silver nanoparticles AgNPs have been proved to be an efficient antimicrobial agent [15].

The current study focuses on the extracellular production of AgNPs using *T. granarium* larval extract for the first time. Following the synthesis of AgNPs, characterization of their properties as well as antibacterial activities against clinical isolate of multidrug-resistant *Salmonella Typhi.*

2. Material and Methods

2.1. *Trogoderma granarium* larvae Sources and Feedstock

In this study, *T. granarium* larvae (approximately 4.5–6 mm in length) were obtained from the College of Agricultural Engineering Science, University of Baghdad, Iraq. The larvae were identified based on morphology and coloration (Figure 1) in the College of Science for Women/University of Baghdad, Baghdad, Iraq.

The culture consisted of 500 g of wheat grains, which were cleaned of impurities and placed in a frozen medium for 72 hours at -20 ºC to be sure that they are free from any other pests . The male and female larvae were transferred to 1 liter glass jars (10 cm in diameter) for rearing to four generations before being used in the experiment. They were covered with Aorquenza cloth held in the place by a rubber band, which allowed proper ventilation but also precluded the entry or exit of insects

The culture was incubated at 27±2°C and 70±10% relative humidity. Diets were used to provide sufficient nutrients as well as a source of carbon for larval growth**.**

2.2. Chemical

Silver nitrate ($AgNO_3$) was obtained from Sigma Aldrich. Bacterial culture media (Nutrient broth, Nutrient agar, Mueller Hinton (MH) agar), Antibiotic susceptibility test to various classes of antibiotics (Ampicillin, Amikacin, Amoxicillin / clavulanic acid, Ceftazidime, Ciprofloxacin, Gentamicin, Levofloxacin and Imipenem) 10 mcg was carried out for S. *Typhi* isolates by disk diffusion method (Kirby-Bauer method) according to [16] and Clinical Laboratory Standard Institute recommendations [17].

Figure (1) *Trogoderma granarium* larvae

2.3. Microorganisms

Salmonella Typhi isolate used in this study was selected out of 36 multidrug-resistant isolates isolated from blood samples of inpatients at the Medical City Hospital in Baghdad. These isolates were identified primarily based on morphological characteristics and biochemical tests, then subjected to Vitek 2 system to confirm the identification.

2.4. Preparation of larval extract

The larval extract was prepared by adding 5 mL of deionized distilled water into a tube containing 100 larvae. The sample was homogenizing for 3 minutes using an ultrasonic device at room temperature, which was capable of destroying larval tissues within less than 3 minutes. To remove the precipitation, the tube was centrifuged at 20,000 rpm for 5 minutes at 4 °C. After that, the supernatant was transferred into a new sterile tube.

2.5. Preparation $AgNO_3$ solution

In 100 ml of deionized distilled water (DW), 16.98 g of silver nitrate was dissolved. Then, 1 ml of the prepared $AgNO_3$ solution was added to another 1000 ml of DW to make 1 mM solution.

2.6. Synthesis of AgNPs

Into 95 ml of 1 mM $AgNO_3$ solution, 5 ml of larval extract was sprinkled. The solutions were sonicated for 20 minutes under ultrasonic conditions, dropwise with a flow rate of 0.2 ml/ min, with an ultrasonic power of 100 watts and a frequency of 42 kHz, and then stirred at 800 rpm at 25°C for 30 minutes before being stored in dark bottles for 24 hours. After 24 hours, the reaction mixture was centrifuged for 10 minutes at 10,000 rpm to obtain a clear supernatant at 4°C, the final colloid samples

were preserved in dark vials. The color of the solution was varied for five days.

2.7. Characterization and Examination of Silver nanoparticles

After getting a stable color change, the solution was centrifuged for 10 min at 5000 rpm to remove any precipitate. The obtained supernatant was centrifuged for another 30 minutes at 12000 rpm. To eliminate any residual larval extract, the pellet then washed three times with deionized DW. The final pellet was resuspended in deionized DW before being used for characterization.

2.7.1. Spectrophotometric analysis

To measure the absorption maxima of the synthesized silver nanoparticles, a spectrum scan in the range of 200-800 nm was performed using a UV-Visible spectrophotometer [18].

2.7.2. Zeta potential

A zeta potential analyzer was used to assess the stability of the synthesized AgNPs in terms of zeta potential (Zeta sizer Nano-ZS90), ranging from -160 mV to +160 mV, and the data was plotted as a graph [19].

2.7.3. Atomic Forced Microscopy (AFM)

A sample of a thin film of nanoparticles (100 µl) was placed on a glass slide and left to dry for 5 min. The slides were then examined using an AFM [20].

2.7.4. Fourier transform infrared spectrometer (FT-IR)

The FT-IR analysis was conducted to evaluate the solution of silver nanoparticles and larval extract at the range of 500-4000 cm=1 region and at 8 cm-1 of a resolution, using Fourier transform infrared spectrometer (Shimadzu). The sample containing synthesized silver nanoparticles (1 mg) was incorporated with KBr (300 mg) to make a hydraulic pellet, which was then pressed and analyzed with FTIR spectroscopy. The occurrence of the peaks was observed with regard to the functional groups in the particles synthesized [18].

2.7.5. Atomic absorption spectroscopy (AAS)

Ag^+ ions concentration in the solution was determined using atomic absorption spectroscopy (GBC 932 AA) over time. Where this measurement can be used to infer the conversion of Ag^+ to Ag0. the sample was withdrawn and centrifuged at 14,000–15,000 rpm during the course of the reaction. The unreacted silver nitrate (Ag^+) in the supernatant solution should be much smaller than Ag0. Thus, the pellets will contain the Ag nanoparticles (Ag0). The amount of Ag^+ ions in the solution of supernatant was then determined using AAS. Because silver precipitation is highly sensitive to the presence of Cl^-, deionized water was utilized in this procedure [21].

2.8. Antibiotics susceptibility test

Antibiotic susceptibility test to various classes of antibiotics (Levofloxacin, Amoxicillin / clavulanic acid, Ciprofloxacin, Amikacin, Ceftazidime, Ampicillin, Imipenem, and Gentamicin) was carried out for *S. Typhi* isolates by disk diffusion method (Kirby-Bauer method) according to [16] and Clinical Laboratory Standard Institute recommendations[17].

2.9. Antibacterial activity assay of AgNPs

The method of agar well diffusion was adopted for assessing the antibacterial activity of the prepared T.g AgNPs against multidrug-resistant *Salmonella Typhi* according to [16]. Mueller Hinton agar was loaded into sterilized Petri plates and let to solidify at room temperature. The fresh bacterial cultures *Salmonella typhi* was swabbed in uniform way over the Mueller Hinton agar plates using a sterile L-shape glass rod. Wells, A sterile cork borer was used to create 4 mm diameter wells in the agar medium. The previously prepared T.g AgNPs solutions (20 µL) were then poured into the corresponding wells. For the control and standard antibacterial agent, the stock solutions of larval extract (without $AgNo_3$) and Penicillin-Streptomycin were used. The loaded plates were incubated for 24 hr at 37c. After incubation, the extent of the produced inhibition zone around the well was measured and determined in mm, demonstrating AgNPs' antibacterial activity. Meanwhile, a UV-Vis spectrophotometer was used to measure the optical density at 600 nm at 5-hour intervals throughout a 45-hour period to evaluate bacterial growth. Freshly grown S. Typhi bacterial cultures with a volume of 180 µL (104 cells/mL) were incubated [22].

2.10. Statistics analysis

Data analysis was carried out by using SPSS V.16 software. The mean, standard error, and the significant differences between values were determined by ANOVA and LSD test [23].

3- Results and discussion

3.1. Synthesis of AgNPs

AgNPs were synthesized using *T. granarium* larval extract and the presence of $AgNO_3$ was detected by a change in the color of the solution. Figure 2 shows how the color of the solution changed from light brown to black, indicating the synthesis of AgNPs. The presence of a black color in the solution shows that silver ions have been reduced to silver [24]. Reduced agents secreted by the bacterium in the solution can catalyze this bio reduction., i.e. *T. granarium* larvae in this work. UV–visible spectroscopy was also used to confirm the

extracellular production of AgNPs. The results of surface plasmon resonance (SPR) revealed that silver nanoparticles smaller than 100 nm were synthesized. This could be due to electron excitation in the conductive band around the nanoparticles' surface [25] [26].

A B

Figure (2) Colour change during the bio reduction of AgNO3 into AgNPs using *T. granarium* larval extract: A: *T. granarium* larval extract, B: AgNO3 solution, and C: Silver nanoparticles.

3.2. Spectrophotometric analysis

UV–visible spectroscopy was utilized to characterize the prepared AgNPs, which is one of the most commonly used and valuable techniques for detecting the synthesis of NPs. Because of light absorption and scattering in the visible range due to plasmon resonance, silver colloids have a variety of colors. The wavelength of resonance is determined by particle size and shape [26].

The bio reduction of silver ions (Ag^+) to silver nanoparticles (Ag^0) was verified by measuring the sample after dilution with a constant volume of deionized water to avoid a high value of absorbance [24], As a blank, deionized water was used.

Silver nanoparticles exhibit important optical properties that are related to localized surface plasmon resonance and are strongly influenced by the nanoparticle morphology [27].

The maximum absorbance peak observed at 385 nm indicated that silver nanoparticles were formed (Figure 3).

Larval extract may contain compounds such as the functional groups of amines, carboxylic acids, and proteins that may be accountable for the bio-reduction of Ag^+ to Ag^0.

Synthesizing AgNPs using larval extract have advantages over other extracts. For example, the AgNPs were found to be stable over 2 years without the addition of any surfactant or pH control to prevent aggregations, while most of the other types of extracts need additives to control aggregations ..

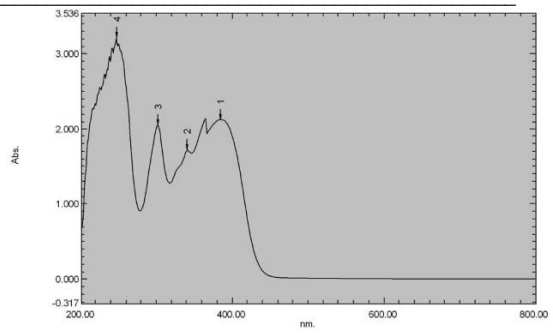

Figure (3) The UV-Vis absorption spectraum of the synthesized silver nanoparticles of larvae extract

3.3. Zeta potential

Figure 4 shows the measurement results of Zeta potential analysis of silver nanoparticles, which recorded a value of -30.78 mV. Zeta potential analysis examines the stability of the nanoparticle's colloid formed in the solution [28]. The negative value of Zeta potential indicated the stability of the AgNPs and that they avoided agglomeration [28]. The Negative Zeta potential value revealed by AgNPs might be attributed to the likely capping of the bio-organic components present in the extract; nevertheless, zeta potential value can be positive or negative [29]. The value that ranges ±0 - 10 mV exhibit a highly unstable colloid, while values of ±10-20 mV, ±20-30 mV, and > ± 30 mV show relatively, moderately, and highly stable colloid, in the respective order [29].

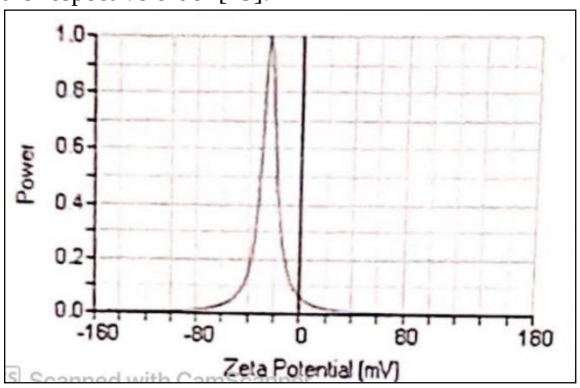

Figure (4) Determination of surface charge of biosynthesized silver nanoparticles by zeta potential

3.4. AFM analysis

AFM images of AgNPs synthesized using silver nitrate and *T. granarium* larval extract are shown in Figure (5). The AgNPs have a spherical form and are evenly dispersed throughout the matrix, as can be seen by AFM images.

According to the histogram of the particles size distribution of AgNPs, the average particle size is around 59 nm.

It was previously unknown that highly stable silver nanoparticles (AgNPs) may be synthesized by bio-reduction of aqueous silver ions (Ag^+) with larval supernatants.

The synthetic process of AgNPs was very fast, where it formed within 5 minutes after the first contact between silver and the larvae cell filtrate. The larvae appear to be able to secrete enzymes that are included in the bio-reduction of Ag^+ [20].

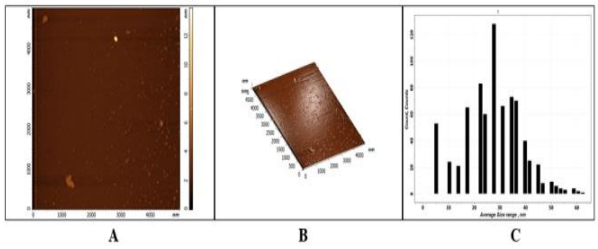

Figure 5. AgNPs produced by the reaction process of $AgNO_3$ solution (1 mM) with larval biomass were imaged using an AFM micrograph. (A) Two-dimensional AFM image of AgNPs. (B) Three-dimensional AFM image of AgNPs. (C) Column AFM diagram of size range of AgNPs

3.5. FTIR spectrum analysis of AgNPs

The use of Fourier transform infrared spectra to observe functional groups involved in the stabilization of synthesized nanoparticles is a an important technique [30].

The interaction of functional groups of larval extract that is involved in the reduction process of $AgNO_3$ and the capping of the subsequently produced AgNPs was confirmed using FTIR spectra of *T. granarium* larval extract and silver nanoparticles. Figure 6 shown the FTIR spectra of *T. granarium* larval extract (Fig 6: A) and AgNPs (Fig 6: B). *T. granarium* larval extract exhibited characteristic stretching frequencies at 1031, 1066, 1321, 1379, 1445, 1492, 1606, 1635, 2850, 2922, 3026, and 3429 cm−1, while the AgNPs expressed visible bands at 1620, 2856, 2926, 3427, and 3446 cm−1. The bands observed at 1620 cm−1 suggest the binding of AgNPs with hydroxyl and carboxyl groups. Also, the bands observed at 3446 cm−1 represent the existence of N–H stretching vibration of amine functional groups. The bands seen at 2856 cm−1 are attributed to O-H stretch vibration of carboxylic acid functional groups. The peaks observed at 2926 cm−1 correspond to the C-H stretch of alkanes functional groups, whereas that at 3427 cm−1 cans be assigned to O-H stretch of alcohols/phenol functional groups. The band at 3446 cm−1 suggests the binding of AgNPs with carboxyl and hydroxyl groups [21].According to the FTIR results, biological molecules may be included in the synthesis and stabilization of AgNPs.

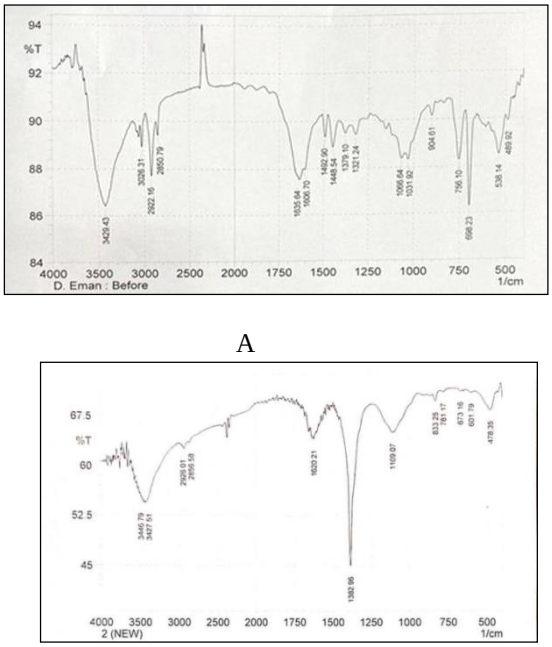

Figure (6) FTIR spectra Results
A: FTIR of *T. granarium* larval extract, B: The FTIR of AgNPs

3.6. Atomic Absorption Spectroscopy (AAS)

After stabilizing the color change of green silver nanoparticle solutions, the concentration of silver ions (Ag^+ ions) in each of the prepared green silver nanoparticle solutions was determined using an AAS. The amount of silver ions in the supernatant solution was determined by AAS. The conversion of Ag^+ to Ag^0 is represented by the rate of reduction in the concentration of Ag^+ ions [21].

Different concentrations of silver nitrate $AgNO_3$ (1, 2, 3, 4, 5, 6 m M) were prepared in DW and a calibration curve was obtained by using it as a standard solution (figure 7). the concentrations were 65 ppm for silver nanoparticles of *T. granarium* larval extracts.

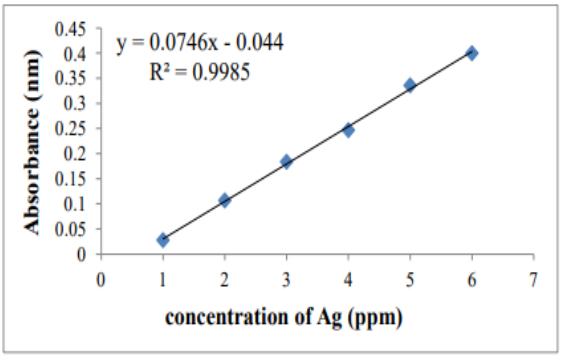

Figure (7) the Standard curve of $AgNO_3$ concentrations for the silver ions concentration determination

3.7. Antibiotics susceptibility test

As shown in Figure (8) according to antibiotics susceptibility test by Kirby-Bauer method, *Salmonella Typhi* isolate exhibited a multi-drug resistant (MDR) pattern that included resistant to Levofloxacin, Ciprofloxacin, Ampicillin, Ceftazidime, Gentamicin, Amoxicillin, Imipenem, and Amikacin.

Over the past decade, several types (strains) of *S. Typhi* have become resistant to many antibiotics [31]. One of the newly emerging strains of Salmonella Typhi that is extensively drug-resistant (XDR) is resistant to all but two classes of antibiotics recommended for treatment (macrolides and carbapenems).

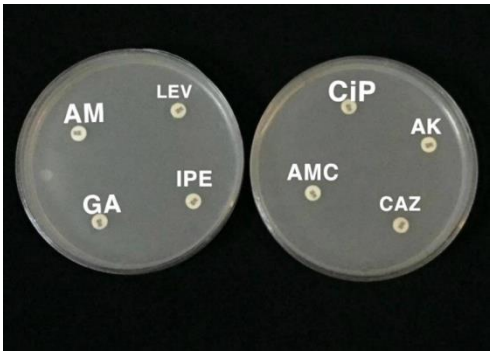

Figure 8. Results of antibiotics susceptibility testing by Kirby Bauer method

3.8. Antibacterial activity assay of silver nanoparticles (AgNPs)

The antibacterial activity results of AgNPs prepared using *T. granarium* larval extract against multidrug-resistant *Salmonella Typhi* using agar well diffusion method shown in Figure (9) indicated that the AgNPs showed inhibiting activities against multidrug-resistant *Salmonella Typhi*.

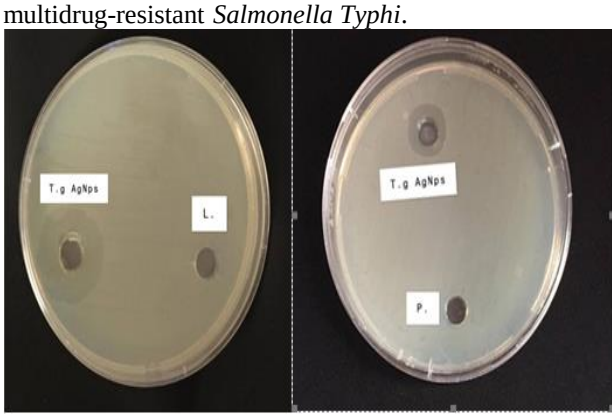

Figure (9): The Antibacterial activity (inhibition zones) of T.g AgNps, Penicillin-Streptomycin (P) and stock solution of larval extract (L) against multidrug-resistant *Salmonella Typhi*.

According to previous research, the formation of inhibitory zones was likely caused by the silver nanoparticles destabilizing the outer membrane, collapsing the plasma membrane, and depleting intracellular ATP [32].

The mechanisms of the bactericidal activities of Ag^0 and AgNPs remains to be comprehended. According to several research, silver has a higher propensity for reacting with phosphorus and sulfur compounds [32]. As is widely known, the cell wall of bacteria contains several sulfur-containing proteins, which may be favored sites for

AgNPs to act. The size of AgNPs ranged from 1–60 nm, on the other hand, Sulfur-containing proteins as well as phosphorus-containing substances like DNA in the cell nucleus can be efficiently reacted with AgNPs [33]. Furthermore, it is also thought that after AgNPs penetrated into the bacterial cell, it inactivates some bacterial enzymes that's are vital for their metabolic activity, generating hydrogen peroxide H_2O_2 and eventually promoting the death of bacterial cells [34]. It was also discovered that the detrimental reactions of AgNPs with DNA induced the latter to lose its ability to replicate and that silver ion treatment rendered cellular proteins inactive [35]. Ag^+ ions in higher concentrations have been found to interact with nucleic acids and cytoplasmic components [36] and affect the metabolic processes of the bacteria such as cell division and cell respiration, finally leading in the cell's death [35] Table 1,2.

Table 1. Inhibition zones revealing the antibacterial activity *T. granarium* AgNPs 65 ppm, Penicillin-Streptomycin, and stock solution of larval extract at 37 °C when implemented on bacterial strains of *Salmonella typhi* (MDR)

No	treatment	Mean ± SE of the Diameter of inhibition zone (mm)	LSD
1	larval extract	0 mm	
2	*T. granarium* AgNPs	17 mm	
3	Penicillin-Streptomycin	0 mm	

Table 2. Optical density OD at 600 nm (in broth) showing the inhibition activity of *T. granarium* AgNPs (T.g AgNps), Penicillin-Streptomycin (P) and stock solution of larval extract (L) when tested on bacterial strain of multidrug-resistant *Salmonella Typhi*.

Salmonella typhi	Antibactrial treatment	Time (h)								
		5	10	15	20	25	30	35	40	45
1	T.g AgNps	0.18	0.22	0.25	0.30	0.35	0.38	0.40	0.35	0.30
2	L	0.20	0.23	0.27	0.33	0.50	0.60	0.73	0.61	0.68
3	P	0.25	0.40	0.88	1.30	1.31	2.48	2.58	2.43	2.20
LSD value		0.118 NS	0.202 NS	0.294 *	0.424 *	0.481 *	0.571 *	0.652 *	0.612 *	0.581 *
* (P≤0.05).										

4- Conclusion

For the first time this work used the aqueous extract of *Trogoderma granarium* larvae to prepare stable silver nanoparticles (AgNPs) using the rapid green approach, where the aqueous extract was utilized as a reducing and capping agent. The results of surface Plasmon resonance at 430 nm in UV–Vis spectra confirm the formation of AgNPs, where the size of the synthesized particles was less than 100 nm.

The analysis of AFM predicted the uniform spherical form of AgNPs along with the particle size distribution within the average of 59 nm. It was previously unknown that highly stable AgNPs could be synthesized by bio-reducing aqueous silver ions (Ag^{+}) with larval supernatants. Furthermore, the abundant sources and low cost of larval extract make them interesting targets for scaling up metallic non-materials to discover different catalytic and biomedical applications.

The result of Antibacterial activity of AgNPs indicated that the AgNPs showed inhibiting activities against multidrug-resistant *Salmonella Typhi.*

The current study demonstrated an effective and low-cost biological methodology for synthesizing metal nanoparticles, which might be helpful in the synthesis of a new antimicrobial agent against pathogenic microorganisms.

5- Funding sources

By another's themselves

6- Conflict of interest

The authors declared no potential conflicts of interest.

7- References:

S. H. Lee and B. Jun, "Silver Nanoparticles : Synthesis and Application for Nanomedicine," Int. J. Mol. Sci., vol. 20, no. 865, pp. 1–23, 2019.

[2] I. Khan, Khalid Saeed, and I. Khan, "Nanoparticles: Properties, applications and toxicities," Arab. J. Chem., vol. 12, pp. 908–931, 2019.

[3] ISO/TS80004-1, "Nanotechnologies — Vocabulary — Part 1: Core terms Table," 2015.

[4] S. Sharmin, M. M. Rahaman, C. Sarkar, O. Atolani, M. Islam Torequl, and O. S. Adeyemi, "Nanoparticles as antimicrobial and antiviral agents: A literature-based perspective study," Heliyon, vol. 7, no. e0645, pp. 1–9, 2021.

[5] I. Ijaz and E. Gilani, "Detail review on chemical, physical and green synthesis, classification, characterizations and applications of nanoparticles," Green Chem. Lett. Rev., vol. 13, no. 5, pp. 223–245, 2020.

[6] Y. T. Gebreslassie and H. G. Gebretnsae, "Green and Cost-Effective Synthesis of Tin Oxide Nanoparticles: A Review on the Synthesis Methodologies, Mechanism of Formation, and Their Potential Applications," Nanoscale Research Letters, vol. 16, no. 97. pp. 1–16, 2021.

[7] A. M. El Shafey, "Green synthesis of metal and metal oxide nanoparticles from plant leaf extracts and their applications: A review," Green Process. Synth. 2020;, vol. 9, pp. 304–339, 2020.

[8] R. Shanmuganathan, I. Karuppusamy, S. Muthupandian, and M. Harshiny, "Synthesis of Silver Nanoparticles and their Biomedical Applications - A Comprehensive Review,"

Curr. Pharm. Des., vol. 25, no. July, pp. 1–11, 2019.

[9] T. Behl et al., "The dichotomy of nanotechnology as the cutting edge of agriculture: Nano-farming as an asset versus nanotoxicity," Chemosphere, vol. 288, Part, no. 132533, pp. 6535–0045, 2022.

[10] M. Godoy-Gallardo et al., "Antibacterial approaches in tissue engineering using metal ions and nanoparticles: From mechanisms to applications," Bioact. Mater., vol. 6, pp. 4470–4490, 2021.

[11] H. Mohammed et al., "Antimicrobial Mechanisms and Effectiveness of Graphene and Graphene-Functionalized Biomaterials. A Scope Review," Front. Bioeng. Biotechnol., vol. 8, no. 465, pp. 1–22, 2020.

[12] J. Ma and K. L. and S. Gu, "Selective strategies for antibacterial regulation of nanomaterials," RSC Adv. Open, vol. 12, pp. 4852–4864, 2022.

[13] W. Linlin, C. Hu, and L. Shao, "The antimicrobial activity of nanoparticles: present situation and prospects for the future," Int. J. Nanomedicine, vol. 12, pp. 1227–1249, 2017.

[14] S. M. Kraemer, O. W. Duckworth, J. M. Harrington, and W. D. C. Schenkeveld, "Metallophores and Trace Metal Biogeochemistry," Aquat. Geochemistry, vol. 21, no. 2–4, pp. 159–195, 2015.

[15] K. Nomiya, A. Yoshizawa, K. Tsukagoshi, N. C. Kasuga, S. Hirakawa, and J. Watanabe, "Synthesis and structural characterization of silver(I), aluminium(III) and cobalt(II) complexes with 4-isopropyltropolone (hinokitiol) showing noteworthy biological activities. Action of silver(I)-oxygen bonding complexes on the antimicrobial activities," J. Inorg. Biochem., vol. 98, no. 1, pp. 46–60, 2004.

[16] A. W. Bauer, W. M. Kirby, J. C. Sherris, and M. Turck, "Antibiotic susceptibility testing by a standardized single disk method.," Am. J. Clin. Pathol., vol. 45, no. 4, pp. 493–496, 1966.

[17] M. P. Weinstein et al., Performance standards for antimicrobial susceptibility testing, 32nd ed. Clinical and Laboratory Standards Institute, 2020.

[18] K. Anandalakshmi, J. Venugobal, and V. Ramasamy, "Characterization of silver nanoparticles by green synthesis method using Pedalium murex leaf extract and their antibacterial activity," Appl. Nanosci., vol. 6, no. 3, pp. 399–408, 2016.

[19] S. Raja, V. Ramesh, and V. Thivaharan, "Green biosynthesis of silver nanoparticles using Calliandra haematocephala leaf extract, their antibacterial activity and hydrogen peroxide sensing capability," Arab. J. Chem., vol. 10, no. 2, pp. 253–261, 2017.

[20] K. Elangovan, D. Elumalai, S. Anupriya, R. Shenbhagaraman, P. K. Kaleena, and K. Murugesan, "Phyto mediated biogenic synthesis of silver nanoparticles using leaf extract of Andrographis echioides and its bio-efficacy on anticancer and antibacterial activities," J. Photochem. Photobiol. B Biol., vol. 151, pp. 118–124, 2015.

[21] M. K. Choudhary, J. Kataria, S. S. Cameotra, and J. Singh, "A facile biomimetic preparation of highly stabilized silver nanoparticles derived from seed extract of Vigna radiata and evaluation of their antibacterial activity," Appl. Nanosci., vol. 6, no. 1, pp. 105–111, 2016.

[22] B. Le Ouay and F. Stellacci, "Antibacterial activity of silver nanoparticles: A surface science insight," Nano Today, vol. 10, no. 3, pp. 339–354, 2015.

[23] S. Rajeshkumar and C. Malarkodi, "In Vitro Antibacterial Activity and Mechanism of Silver Nanoparticles against Foodborne Pathogens," Bioinorg. Chem. Appl., vol. 2014, 2014.

[24] K. Kalimuthu, R. Suresh Babu, D. Venkataraman, M. Bilal, and S. Gurunathan, "Biosynthesis of silver nanocrystals by Bacillus licheniformis," Colloids Surfaces B Biointerfaces, vol. 65, pp. 150–153, 2008.

[25] X. F. Zhang, Z. G. Liu, W. Shen, and S. Gurunathan, "Silver nanoparticles: Synthesis, characterization, properties, applications, and therapeutic approaches," Int. J. Mol. Sci., vol. 17, no. 1534, 2016.

[26] K. K. Paul and P. K. Giri, "Plasmonic metal and semiconductor nanoparticle decorated TiO2-based photocatalysts for solar light driven photocatalysis," Encycl. Interfacial Chem. Surf. Sci. Electrochem., pp. 786–794, 2018.

[27] S. Samimi, N. Maghsoudnia, R. B. Eftekhari, and F. Dorkoosh, Lipid-Based Nanoparticles for Drug Delivery Systems, 1st Editio. Elsevier Inc., 2018.

[28] B. Chakraborty et al., "Evaluation of antioxidant, antimicrobial and antiproliferative activity of silver nanoparticles derived from Galphimia glauca leaf extract," J. King Saud Univ. - Sci., vol. 33, no. 8, pp. 1–23, 2021.

[29] A. Dutta, Fourier Transform Infrared Spectroscopy. Elsevier Inc., 2017.

[30] M. K. Bin Bakri, M. R. Rahman, P. L. N. Khui, E. Jayamani, and A. Khan, Use of sustainable polymers to make green composites, no. 3. LTD, 2021.

[31] H. M. El Shora, A. M. El Shobaky, and H. S. Al Hayanni, "Characterization of β-Lactamase from Two Pathogenic Bacteria," Int. J. Curr. Microbiol. Appl. Sci., vol. 6, no. 6, pp. 927–941, 2017.

[32] A. Simon-Deckers et al., "Size-, composition- and shape-dependent toxicological impact of metal oxide nanoparticles and carbon nanotubes toward bacteria," Environ. Sci. Technol., vol. 43, no. 21, pp. 8423–8429, 2009.

[33] S. Kittler, C. Greulich, J. Diendorf, M. Köller, and M. Epple, "Toxicity of silver nanoparticles increases during storage because of slow dissolution under release of silver ions," Chem. Mater., vol. 22, no. 16, pp. 4548–4554, 2010.

[34] Z. Ferdous and A. Nemmar, Health impact of silver nanoparticles: A review of the biodistribution and toxicity following various routes of exposure, vol. 21, no. 2375. 2020.

[35] W. R. Li et al., "A comparative analysis of antibacterial activity, dynamics, and effects of silver ions and silver nanoparticles against four bacterial strains," Int. Biodeterior. Biodegrad., vol. 123, pp. 304–310, 2017.

[36] P. Urwade et al., "EPA Public Access," J. Antibiot. (Tokyo)., vol. 727, no. 1, pp. 50–53, 2019.